J. Chem. Sci. (2020)132:71
https://doi.org/10.1007/s12039-020-01773-6

REGULAR ARTICLE

Investigation on the structural, thermal and hydration properties of gold-fullerene nanocomposite

G JAYABALAJI[a], L RAMYA[b] and J MEENA DEVI[a,*]
[a]Centre for Nanotechnology and Advanced Biomaterials and School of Electrical and Electronics Engineering, SASTRA Deemed University, Thanjavur 613 401, Tamilnadu, India
[b]School of Chemical and Biotechnology, SASTRA Deemed University, Thanjavur 613 401, Tamilnadu, India
E-mail: jmeenadevi@sastra.ac.in

MS received 26 September 2019; revised 29 December 2019; accepted 12 January 2020

Abstract. In this article, we report the self-assembly process, structural features, thermal and hydration properties of the gold fullerene nanocomposite at room temperature by applying molecular dynamics simulation technique. The gold-fullerene systems constituting alkanethiol capped gold nanoparticle and pristine fullerene in explicit water have been simulated to gain insights on the influence of the terminal methyl (hydrophobic) and hydroxy (hydrophilic) groups on their structure and properties. The physisorption of the fullerene molecule into the thiol layer of the gold nanoparticle has been demonstrated and elucidated. The chemical functionality of the terminal groups was found to affect the structure, specific heat capacity and the wetting behavior of the gold-fullerene nanocomposite. The findings from this computational study may aid the understanding and development of novel gold-fullerene nanostructures for modulating their structural, thermal and hydration properties through the modification of their surface functional groups.

Keywords. Gold nanoparticle; fullerene; nanocomposite; molecular dynamics simulation.

1. Introduction

The unique and versatile properties of the gold nanoparticles such as stability, ease of surface functionalization, biocompatibility, biomolecular interactions, surface plasmon resonance, fluorescence, electrical conductance, chemical reactivity and redox behavior, make them an important, fascinating and promising candidate in the field of nanoscience and technology.[1–4] The properties and functions of the gold nanoparticles can be modified by altering their size, geometric shape, surface area, capping agents, morphology, solubility, surrounding environment and so on.[5–8] Gold nanoparticles have potential applications in the diverse fields such as electronics, optics, medical imaging, biological labelling, cancer therapy, targeted drug delivery, diagnostics, catalysis, chemical sensors and biosensors.[1,2,9–13]

Fullerene has received prime attention in the scientific community due to its characteristic symmetrical hollow structure, smaller size, electrical, mechanical, photo-optical, photochemical, electrochemical, antioxidant, and biological properties.[14–18] C_{60} fullerene molecule has an appealing close caged hollow structure resembling a soccer ball. It consists of a network of sixty sp^2-hybridized carbon atoms in the shape of truncated icosahedron composed of twelve pentagons and twenty hexagon rings. The distinctive structure and properties of fullerene make them applicable in imaging, radiotherapy, anti-HIV activity, free-radical scavenging, specific DNA cleavage, drug delivery, optoelectronics, electronic devices, sensors and photovoltaics.[18–22]

Gold nanoparticles and fullerene are rich, unique and extraordinary in their properties and functionalities. Hence, their combination may emerge as a wonderful nanoscale assembly offering a multitude of

*For correspondence

Electronic supplementary material: The online version of this article (https://doi.org/10.1007/s12039-020-01773-6) contains supplementary material, which is available to authorized users.

Published online: 03 June 2020

desired and novel properties which may meet the needs, demands and advances of the biological and technological applications. In the literature, synthesis, properties and applications of the gold-fullerene nanocomposite with the different linking and capping molecules have been reported.[23–31] Gold-fullerene nanocomposite has been reported to have improved, significant electrochemical response, electro-catalytic activity, optical limiting effect, surface plasmon resonance, fluorescence quenching, surface-enhanced Raman scattering, photo-dynamic therapeutic efficacy and self-cleaning super-hydrophobicity. These improved and significant attributes of gold-fullerene nanocomposite demonstrate their potential for electrochemical, spectroscopic and optical sensing, catalytic and tumor diagnostic applications.[23–31]

Some simulation work has been reported in the literature for the gold-fullerene systems focusing on their structural, mechanical, sensing, magnetic, spectroscopic, electronic and thermoelectric properties.[32–45] The chemisorption and motion of fullerene on gold substrate has been reported from DFT and MD simulation studies.[32–36] Ahangari *et al*.,[32] have studied the adsorption of fullerene-wheeled nanocar onto a gold substrate using the density functional theory (DFT) simulations. They have determined the binding energy between the nanocar and gold substrate to be −217.45 kcal/mol and the net charge transfer from the nanocar to the gold substrate to be about 9.56 electrons.[32] Ryu *et al*.,[37] have identified the origin of the molecular rectification of fullerene derivative assembled on a gold surface using a multi-scale molecular modeling approach combining MD, DFT and non-equilibrium Green's function (NEGF) calculations. They have ascribed the molecular rectification to the coupling of controlled molecular motion and asymmetric electron transport.[37] Sutradhar *et al*.,[44] have designed and synthesized gold nanocomposite based on DL-homocysteine functionalized fullerene. They have determined the electrochemical sensing activity of this composite-modified glassy carbon electron (GCE) towards L-histidine from their experimental studies. They have reported the charge transfer interaction between the analyte histidine and the composite from their molecular dynamics simulation studies.[44]

Many of the reported computational investigations on the gold-fullerene systems in the literature have been done on a gold surface and few simulation studies have been done on smaller size gold clusters. In the present work, we have performed the molecular dynamics simulations of the alkanethiol capped gold nanoparticle and fullerene in an aqueous medium to study their self-assembly, structure, specific heat capacity and their interaction with water. The objective of the present simulation study is to investigate the influence of the terminal group functionality on the structural, thermal and hydration properties of this gold-fullerene nanocomposite and to explore their structure-property relationship.

The extensive research and detailed study on the design and development of the novel nanohybrid systems are very essential as they display synergistic effect and their superior properties and functions may be tailored to match the requirements of chemical, technological and biological applications. The size of the nanoparticles lies in the range of biological molecules such as lipids, proteins, enzymes, DNA and RNA. The gold nanoparticles and fullerene exhibit good bio-compatibility and remarkable optical, electronic, mechanical and chemical properties and biological activity. So the nanoscale assembly constituting biocompatible metallic gold nanoparticle and semi-conducting fullerene may be designed and developed as a multi-functional material, which may be used as a component for building nanoscale electronic, sensing, imaging devices, robots, biological interface, biological probe, bio-materials, targeted drug delivery system, therapeutic agent and diagnostic tool. The knowledge on the thermal properties of the gold-fullerene nanocomposite is important for developing devices in the industrial, chemical, biological and engineering applications involving thermal stability, thermal process and heat transfer.

As the gold nanoparticles and fullerene are being widely used in nanoscience, catalysis, biomedicine and biotechnology, a detailed study on their interactions with biological fluids at the molecular level is vital. The electrochemical and biological applications of the gold-fullerene nanocomposite depend on their surface functional group, surface chemistry, surface properties, water-mediated interactions, and on their behaviour in the aqueous environment. The pristine gold nanoparticles and fullerene are hydrophobic in nature. The hydrophobic or hydrophilic nature of the terminal group of capping alkane thiol layer of gold nanoparticle will influence the solubility and the surface interactions of the gold-fullerene nanocomposite with the surrounding water environment. The wetting behavior of the nanostructure is of great importance in applications such as bio-sensors, catalysts, lubrication, protein adsorption, drug delivery, biological interface, molecular recognition and electro-mechanical systems. So, good knowledge and comprehensive understanding of the interactions between the gold-fullerene nanostructure and the surrounding water molecules at the molecular level is essential both from the

application and fundamental science perspective. Hence in our present simulation study, we have employed molecular dynamics simulation method to study the structural, thermal and hydration properties of the methyl gold-fullerene system and hydroxy gold-fullerene system.

2. Computational details

We have constructed two systems, one comprised of methyl terminated alkanethiol capped gold nanoparticle & fullerene (C_{60}), and the second one comprised of hydroxy-terminated alkanethiol capped gold nanoparticle & fullerene (C_{60}). These systems were solvated in water box of TIP3P[46] water model. The shape of the gold core is approximately spherical and it contains 249 gold atoms. This gold core is taken from the FCC lattice of bulk gold. The size of the gold core calculated using the radius of gyration is 7.8 Å. This gold core was capped by a monolayer of 86 alkanethiol chains of the chemical composition of S–$[CH_2]_{12}$–X, where X is the terminal group, which can be either a methyl (hydrophobic) or hydroxy group (hydrophilic). The capping alkanethiol chains were distributed randomly on the surface of the gold core set in trans configuration with their sulphur head groups perpendicular to the gold surface and attached in atop position. The united atom model has been employed for the methylene and methyl groups.

In the initial configuration, center of mass (COM) distance between the gold core and fullerene was around ~30 Å. The initial configuration of the gold-fullerene systems solvated in water box has been built using the following steps. In the first step, functionalized gold nanoparticle and fullerene have been subjected to energy minimization individually. In the second step, they were combined and this combined system was minimized. In the final step, minimized gold-fullerene system was immersed in the water box and the energy minimization was performed for the solvated gold-fullerene systems. This minimized starting structure is then subjected to molecular dynamics simulation run.

Heinz *et al*.,[47] Lennard Jonnes (LJ) potential parameters have been applied for the gold atoms of the gold core. The force field parameters for the alkanethiol chains were taken from the literature[48,49] and they are given in detail in our previous work.[50] The force field parameters for the fullerene carbon atoms were taken from the aromatic carbon atoms of the CHARMM27 force field.[51] Heinz *et al*.,[47] LJ interaction parameters for the gold atoms and CHARMM27 force field parameters for the fullerene carbon atoms have been reported to yield significant results in the literature for the gold systems[52–54] and fullerene systems,[55–57] respectively. Perfilieva *et al*.,[52] have applied LJ potential to the gold atoms to study the structure of the citrate capped gold nanoparticles. Giri and Spohr[53] have employed LJ potential to model the interaction for gold to investigate the influence of chain length on the structure of the thiol capped gold nanoparticles in the aqueous NaCl solution. Velachi *et al*.,[54] have employed LJ potential for the gold atoms to study the structure and hydration properties of the mixed self-assembled monolayer coated gold nanoparticles.

Kraszewski *et al*.,[55] have employed CHARMM27 forcefield parameters for the fullerene molecules to investigate their interactions with the potassium channels. Yesylevskyy *et al*.,[56] have used CHARMM27 forcefield parameters for the functionalized fullerene to study the translocation of fullerene molecules through the model membrane. Sun *et al*.,[57] have applied CHARMM27 forcefield parameters for the fullerene to investigate the effects of surface roughness on hydrophobic interactions. Hence the approach of modelling the interactions between gold atoms using LJ potential and fullerene carbon atoms using CHARMM27 forcefield parameters in the present simulation study can yield correct description for the structure and properties of the gold-fullerene nanocomposite.

Molecular dynamics (MD) simulation technique has been employed to investigate the structure and properties of the gold-fullerene nanocomposite. All the molecular dynamics simulations have been performed in the NPT ensemble at a pressure of 1.013 bar and a temperature of 300 K using the NAMD package.[58] The systems have been minimized for 3000 steps using the conjugate gradient energy minimization method. Langevin dynamics has been used with a damping coefficient of 5/ps for temperature control. Periodic boundary conditions have been imposed and the size of the simulation box is 94 × 87 × 85 Å. A cutoff distance of 12 Å was used for the non-bonded van der Waals interactions. The particle mesh Ewald method has been applied to calculate the long-range electrostatic interactions. The hydrogen bonds have been fixed using SHAKE algorithm. The integration time step has been chosen as 2 fs and the two systems have been run for a period of 60 ns. The water molecules within 3.5 Å and 6 Å of the gold-fullerene nanocomposite have been considered as Region_1 and Region_2, respectively.

3. Results and Discussion

The main results of this simulation study are (i) The van der Waals force has driven the physisorption of fullerene into the thiol layer of the gold nanoparticle. (ii) The structural features of the gold-fullerene nanocomposite such as size, interparticle distance, organization and conformation of the thiol chains, location of fullerene, mobility of the component molecules have been determined and discussed. The specific heat capacity of the hydroxy gold-fullerene nanocomposite is found to be higher than the methyl gold-fullerene nanocomposite. (iii) The hydroxy gold-fullerene nanocomposite has higher wettability than the methyl gold-fullerene nanocomposite. (iv) The chemical functionality of the terminal groups has influenced the structural, thermal and hydration properties of the gold fullerene nanocomposite. These results were extracted from the analysis of interaction energy, radial density profile, center of mass distance, the radius of gyration, distribution of intermolecular angle and length of the thiol chains, root mean square deviation (RMSD), radial distribution function, hydration shell, hydrogen bonds, orientation of water molecules, water residence time and solvent accessible surface area (SASA).

3.1 *Self-assembly*

Molecular Dynamics Simulations of the methyl and hydroxy, gold-fullerene systems have been carried out under NPT ensemble for a period of 60 ns at room temperature to investigate their structure and properties. The final configurations of the two gold-fullerene nanohybrid systems obtained from the molecular dynamics simulation are shown in Figure 1. The intermolecular interactions between gold nanoparticle and fullerene molecule in water solvent have resulted in the formation of stable gold-fullerene nanocomposite in both the methyl and hydroxy systems. In both the nanocomposite, fullerene molecule has got adsorbed into the thiol layer of the gold nanoparticle.

The interaction energy between thiol capped gold nanoparticle and fullerene is presented as a function of time in Figure 2. The van der Waals interactions between thiol capped gold nanoparticle and fullerene have driven the formation of gold-fullerene nanocomposite and so the fullerene molecule has been incorporated into the functionalized surface of the gold nanoparticle. The difference in the time of formation of the methyl and hydroxy, gold-fullerene nanocomposite can be observed from Figure 2. The interaction energy in Figure 2 has started decreasing at 5 and 31 ns for hydroxy and methyl systems respectively. This reveals the time of formation of the nanocomposite, which is around 5 ns for hydroxy system while it is around 31 ns for methyl system. The adsorption of fullerene has happened around 5 ns for hydroxy system, while it has happened around 31 ns for methyl system. The conformational change of the gold-fullerene nanostructure is reflected as a decrease in the interaction energy. The physisorption of fullerene into the surface of the thiol capped gold nanoparticle has caused the energy penalty and hence there is a drop in the interaction energy around 5 and 31 ns for the hydroxy and methyl systems respectively. The radial

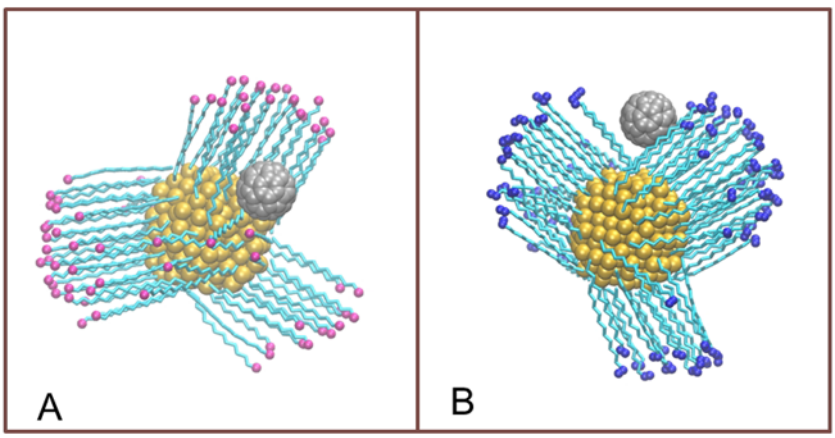

Figure 1. Final configuration of gold-fullerene nanocomposite (a) Methyl (b) Hydroxy. Gold atoms are shown in yellow ochre color in van der Waals representation; alkanethiol chains are shown in light blue color in Licorice representation; Terminal groups are shown in pink (methyl)/dark blue (hydroxy) in Beads representation; Fullerene carbon atoms are shown in gray color in van der Waals representation; Water molecules are not shown for the sake of clarity.

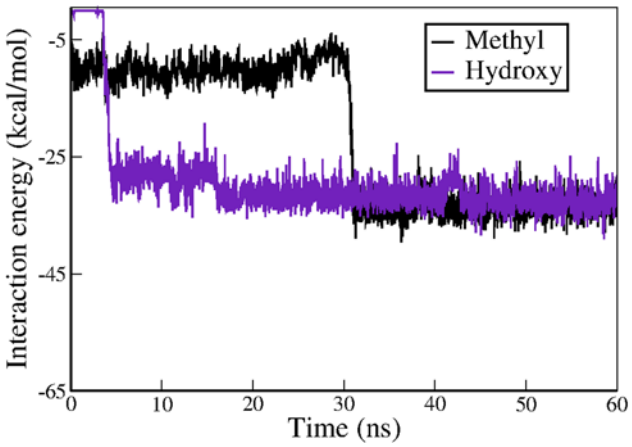

Figure 2. Interaction energy between alkanethiol capped gold nanoparticle and fullerene.

density profile of the final structure of the methyl and hydroxy gold-fullerene nanostructure is plotted as a function of distance from the center of mass of gold core (Figures S1-S2, Supplementary Information). The physisorption of fullerene into the thiol layer of the gold nanoparticle can be evidenced from the radial density profile.

We propose the following mechanism for the self-assembly of gold nanoparticle and fullerene in water. Non-polar fullerene molecule repels the vicinal polar water molecules due to the hydrophobic force and it starts moving toward the gold nanoparticle and gets adsorbed on the gold surface due to the van der Waals interactions between them. In the case of the hydroxy system, the process of self-assembly is governed by the interactions among the hydrophobic fullerene, gold core, and the amphiphilic thiol chains which have hydrophobic head groups, body segments and hydrophilic terminal groups and the water molecules. So the strength of the interactions between the fullerene and capping chains is different near the polar terminal groups and near the non-polar head group, body segments. In the aqueous environment, the interaction between the non-polar fullerene molecule is minimum near the polar terminal hydroxy groups and so the fullerene ball moves into the surface of the functionalized gold nanoparticle and gets adsorbed there due to van der Waals force.

In the case of methyl system, the process of self-assembly is dictated by the interactions among the hydrophobic fullerene, gold core, hydrophobic thiol chains which are completely hydrophobic from the head, body to the terminal segments and the water molecules. The non-polar entities show pronounced affinity in the presence of water due to the hydrophobic effect and so they self-assemble together to minimize their contact with water. This short-range attractive interaction promotes the physisorption of fullerene. The solvent water molecules influence the attraction between the non-polar molecules.

To probe the role of water in the formation of the gold-fullerene nanocomposite, the interaction energy between gold-fullerene nanocomposite and water is plotted as a function of time in Figure 3. The interaction energy of the hydroxy gold-fullerene nanocomposite is lower than the methyl gold-fullerene nanocomposite. This reveals the stronger interactions between the hydroxy system and water than methyl system and water. The aqueous environment has facilitated the rapid formation of the hydroxy gold-fullerene nanocomposite.

We have next investigated the total interaction energy of the gold-fullerene nanocomposite to determine their stability. The total interaction energy (IE) of the gold–fullerene nanocomposite has been determined by subtracting the energy of the individual components such as thiol capped gold nanoparticle (E_{AuNP}) and fullerene ($E_{fullerene}$) from the energy of the nanocomposite (E_{NC})

$$IE = E_{NC} - (E_{AuNP} + E_{fullerene}) \quad (1)$$

The total interaction energy values of the methyl and hydroxy, gold-fullerene nanocomposite estimated using equation (1) are −313.81 and −324.42 kcal/mol, respectively. The fullerene molecule is glued to the alkanethiol capped gold nanoparticle due to the non-bonded interactions between them. The total interaction energy of the hydroxy gold-fullerene nanocomposite is relatively more negative than methyl gold-fullerene nanocomposite and this implies hydroxy gold-fullerene nanocomposite is relatively more stable.

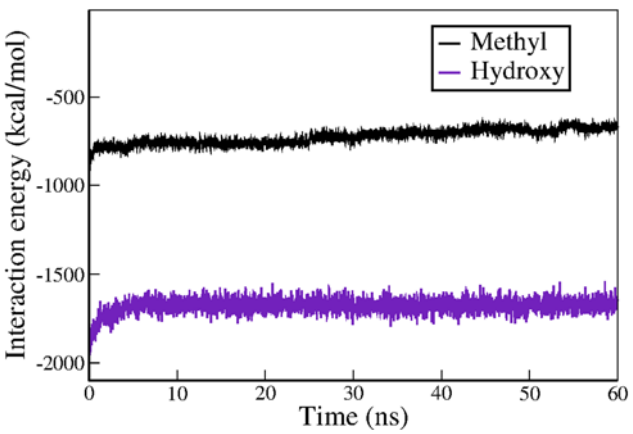

Figure 3. Interaction energy between gold-fullerene nanocomposite and water.

3.2 *Structural characterization*

In this section, the structure of the gold-fullerene nanocomposite has been characterized using center of mass distance (COM), the radius of gyration, radial distribution function, distribution of intermolecular angle and length of thiol chains, RMSD (root mean square deviation) calculations. To examine the movement of the fullerene with respect to the gold core, and to evaluate the distance between the gold core and fullerene, COM distance between the gold core and fullerene has been plotted as a function of time in Figure 4. As expected, similar to the time variation of the interaction energy between the thiol capped gold nanoparticle and fullerene, COM distance of the hydroxy and methyl, gold-fullerene systems become stable around 5 and 31 ns respectively and it remains constant throughout the simulation. This behavior confirms the formation of the gold-fullerene nanocomposite and the constant distance denotes the reduced mobility of fullerene and the adsorption of fullerene on the surface of the gold nanoparticle. Fang *et al.*,[23] have reported the adsorption behavior of fullerene on aqueous gold colloid from their surface-enhanced Raman spectroscopy (SERS) measurements. The average COM distance between the gold core and fullerene calculated from the last 10 ns of the simulation for the methyl and hydroxy, gold-fullerene nanocomposite is 18.49 and 18.62 Å respectively (Table 1). There is no much difference in the COM distance between the gold core and fullerene with respect to the terminal functional groups.

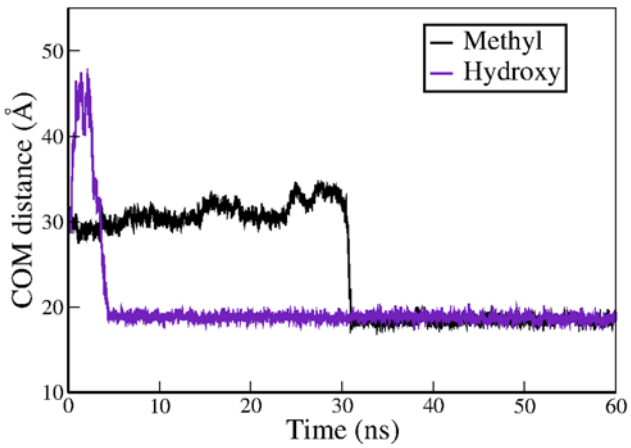

Figure 4. Centre of mass distance between gold core and fullerene.

The size of the gold-fullerene nanocomposite has been observed from the time evolution of radius of gyration shown in Figure 5. Similar to the time variation of COM distance, the size of the hydroxy and methyl, gold-fullerene systems become stable around 5 and 31 ns respectively and it remains constant throughout the simulation. The average size of the methyl and hydroxy gold-fullerene nanocomposite measured using the radius of gyration from the last 10 ns is 17.49 and 17.75 Å respectively (Table 1). Similar to the observation in the COM distance, here also, there is no much change in the size of the gold-fullerene nanocomposite with respect to the terminal functional groups. Fujihara *et al.*,[59] have reported the size range of fullerene thiolate functionalized gold nanoparticles to be around 20 Å from their transmission electron microscopy (TEM) measurements.

To understand the organization of the thiol chains, distribution of the intermolecular angle of the thiol chains is displayed in Figure 6, for both the initial and final configurations of the gold-fullerene nanocomposite. The intermolecular angle is defined as the angle between the end-to-end vectors of the thiol chains. In the initial configuration, thiol chains are randomly oriented and this is manifested as a single broad peak in Figure 6. The presence of multiple peaks in the final configuration signifies the preferential ordered orientation of the thiol chains as molecular bundles. The thiol chains tilt together to form the molecular bundles due to the inter-chain van der Waals interactions.[53]

The depth of penetration of the fullerene into the thiol layer can be quantified from the radial distribution function (RDF) plot between the terminal

Table 1. Structural and thermal properties of gold-fullerene nanocomposite.

Sl. No	Parameter	Methyl	Hydroxy
1	Center of mass distance between gold core and fullerene (Å)	18.49 ± 0.34	18.62 ± 0.36
2	Size of nanocomposite (Å)	17.49 ± 0.03	17.75 ± 0.05
3	Length of thiol chains (Å)	16.97 ± 0.04	16.64 ± 0.06
4	RMSD of gold core (Å)	0.31 ± 0.06	0.23 ± 0.01
5	RMSD of sulphur (Å)	0.62 ± 0.09	0.51 ± 0.05
6	RMSD of terminal group (Å)	2.37 ± 0.29	3.05 ± 0.29
7	RMSD of fullerene (Å)	0.08 ± 0.01	0.09 ± 0.01
8	Specific heat capacity (kcal/mol/K)	5.21 ± 0.41	6.52 ± 0.26

groups and fullerene shown in Figure 7. The major peak around 15.5 Å in both the methyl and hydroxy, gold-fullerene nanocomposite in Figure 7 indicates the most probable distance between the terminal groups and fullerene. This observation suggests the deep adsorption of the fullerene ball into the thiol layer of the gold nanoparticle. In the literature, Bończak *et al*.,[60] have reported the distance from the sulfur atom to the middle of the fullerene ball to be about 9.5 Å from their experimental investigation of gold nanoparticles functionalized with fully conjugated fullerene.

In Figure 7, even though the peak position is the same for both the methyl and hydroxy system, there is a difference in the peak pattern. This different peak behaviour arises as the hydroxy thiol chains bend slightly during the course of dynamics while the methyl thiol chains stand erect. This can be observed from Figure 8 which shows the distribution of thiol chain length. In the water medium, the repulsive hydrophobic interactions between the hydrophobic methyl terminal groups and the water molecule resulting in the erect methyl thiol chains. But in the case of the hydroxy system, the attractive hydrophilic interactions between the hydrophilic hydroxy groups and the water molecules induce the bending of the hydroxy thiol chains.

Moreover, in the case of the methyl system, both fullerene and methyl terminal groups are hydrophobic in nature. But in the case of the hydroxy system, fullerene is hydrophobic in nature while the hydroxy terminal groups are hydrophilic in nature. So there is a difference in the nature of the interaction between the terminal groups and fullerene. From Figure 9, we can see one solvation shell for the methyl system, whereas the hydroxy system has two solvation shells. These differences might have caused different peak behaviour.

The conformation of the alkanethiol chains has been assessed from the distribution of their end-to-end distance presented in Figure 8. In Figure 8, we can see one tall peak centered at 16.9 Å for the methyl system. This single tall peak of the methyl system indicates the extended conformation of the hydrophobic thiol chains as they repel the water molecules. Whereas in the hydroxy system, we can see two peaks. Among these two peaks, one is tall with the center at 16.8 Å and other one is short with the center at 16.0 Å. This short and small peak of the hydroxy system denotes the population of the shorter length thiol chains. Hydroxy system has shorter length chains as they bend due to their affinity towards the water molecules.

The length of the hydroxy-terminated thiol chains varies from 14.9–17.2 Å, while the length of the methyl

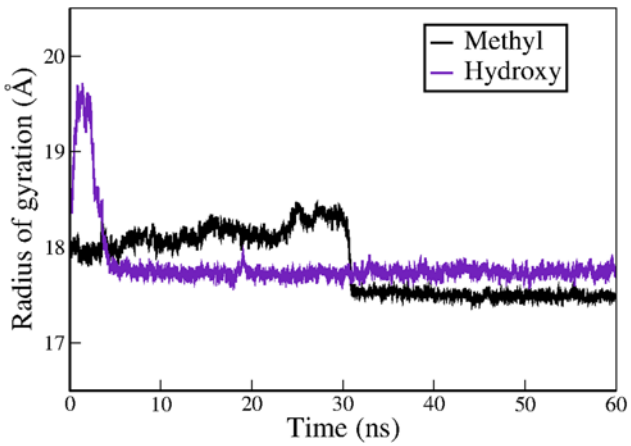

Figure 5. Radius of gyration of gold-fullerene nanocomposite.

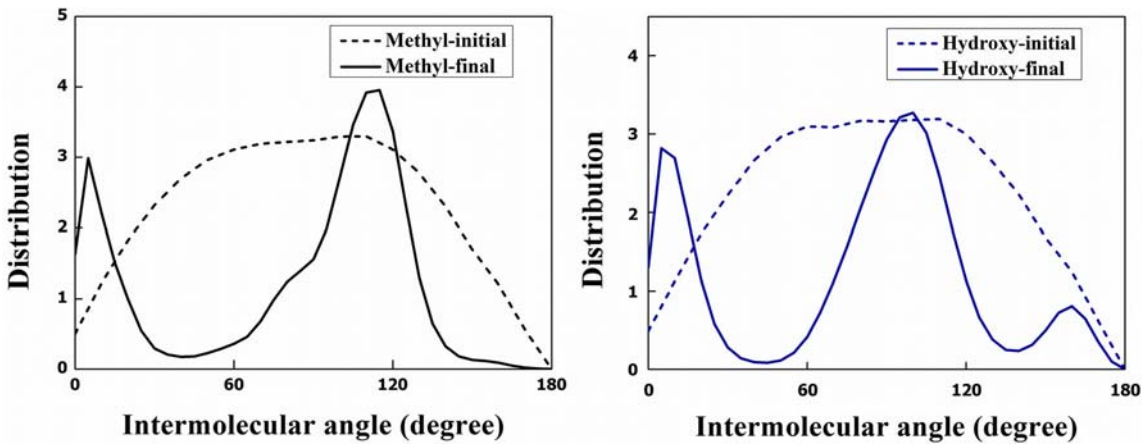

Figure 6. Intermolecular angle distribution of alkane thiol chains.

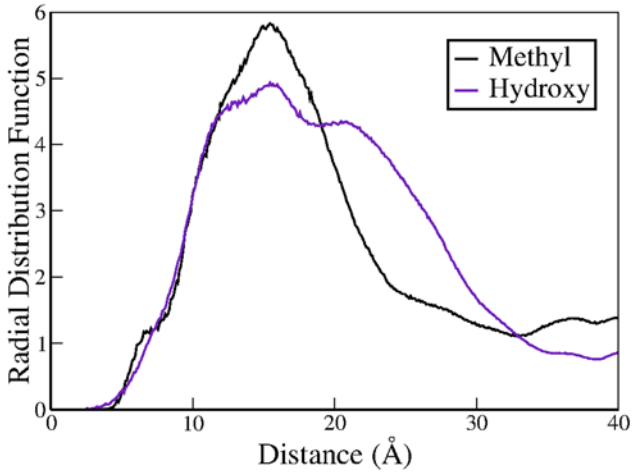

Figure 7. Radial distribution function between terminal groups and fullerene.

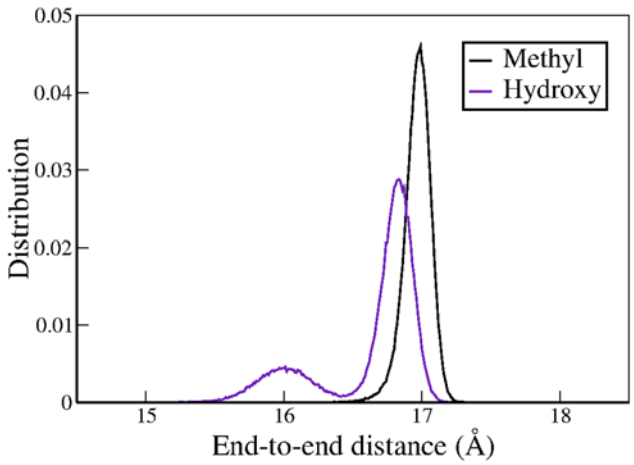

Figure 8. End-to-end distance distribution of alkanethiol chains.

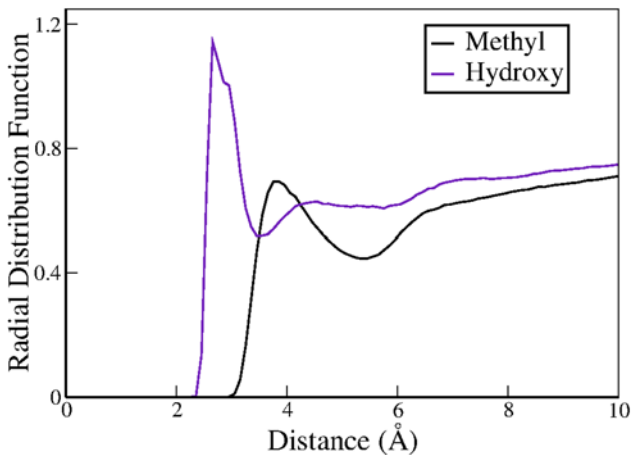

Figure 9. Radial distribution function between the terminal group and water oxygen.

terminated thiol chains varies from 16.1–17.3 Å. This difference is small, as the length of the terminal segments considered in this study is small. The average length of the methyl and hydroxy-terminated thiol chains is 16.97 and 16.64 Å, respectively (Table 1). Velachi *et al.*,[61] have studied the structural properties of mixed self-assembled monolayers of hydrophilic and hydrophobic alkylthiols, with two different chain lengths on gold nanoparticle. They have calculated the end-to-end distance distribution of the thiol chains and they have found that the longer thiol chains with the hydrophilic (carboxyl) terminal groups to be more bent than the longer thiol chains with the hydrophobic (methyl) terminal groups.

The mobility of the fullerene molecule, gold core, sulphur (head group) and terminal groups have been quantitatively elucidated by the average root mean square (RMSD) values calculated from the last 10 ns of the simulation and they are given in Table 1. The RMSD values of the fullerene molecules are 0.08 and 0.09 Å for the methyl and hydroxy systems, respectively. The smaller fluctuation in the position of the fullerene molecules is a signature of their strong adsorption, stability and hindered movement as they are bound to the gold nanoparticles. Yu *et al.*,[62] have reported that the RMSD value of fullerene as 0.15 Å from their simulation studies on binding effects of fullerene-based molecules to tyrosine phosphatase. Balamurugan *et al.*,[63] have reported that the RMSD value of fullerene as 0.10 Å from their simulation studies on carotene-porphyrin-fullerene molecular triad in explicit tetrahydrofuran (THF) solvent.

The mobility of the terminal groups is important for the applications involving targeted interactions with the biological molecules. The RMSD values of the methyl and hydroxy terminal groups are 2.37 and 3.05 Å, respectively. The mobility of the hydroxy moieties is higher than the methyl moieties. This flexibility arises from the favorable hydrophilic interactions between the terminal hydroxy moieties and the water molecules. This result is consistent with the distribution of the length of thiol chains observed in Figure 8. Some of the hydroxy-terminated thiol chains were found to have shorter chain length. This can be associated with their bent structure and a relatively higher degree of mobility.

The mobility of the sulphur head group is lesser than the terminal groups as they are strongly bonded to the gold atoms. The RMSD values of the gold core of the methyl and hydroxy systems are 0.31 and 0.23 Å, respectively. As expected, the flexibility of the gold atoms is lesser than the sulphur head group and the terminal group as the mass of the gold atoms is very much heavier and they remain intact in the gold core as a stable nanoparticle.

3.3 *Specific heat capacity*

The estimation of the specific heat capacity value of the nanocomposite material is essential for designing the biomedical,[64] biochemical, thermal, optical, electronic and industrial components. The specific heat capacity is a fundamental macroscopic physical quantity related to the vibrations at the microscopic level. The specific heat capacity (C) is usually defined in terms of mean square fluctuations of the energy.

$$C = \frac{\langle E^2 \rangle - \langle E \rangle^2}{k_B T^2} \quad (2)$$

The specific heat capacity values of the methyl and hydroxy, gold-fullerene nanocomposite calculated using the above equation are 5.21 and 6.52 kcal/mol/K, respectively and they are given in Table 1. The value of the specific heat capacity of the hydroxy gold-fullerene nanocomposite is higher than the methyl gold-fullerene nanocomposite. In general, specific heat capacity value of any given substance depends on various factors like chemical composition, number of atoms, molecular weight, density, impurities, molecular structure, number of degrees of freedom, lattice vibrations, phonon density and temperature. There is a difference in the molecular weight of hydroxy and a methyl group. As the molecular weight of the hydroxy group is slightly higher than the methyl group, the specific heat capacity value of the hydroxy gold-fullerene nanocomposite may be slightly higher. The methyl terminated chains have extended conformation while some of the hydroxy-terminated chains have bent structure. The longer chain will lower the frequency of the oscillation and so methyl gold-fullerene nanocomposite may have relatively lower specific heat capacity value.

Sauceda *et al*.,[65] have calculated the low-temperature specific heat of gold nanoparticles from the vibrational density of states and they have observed small variation in the specific heat with respect to the size and shape of gold nanoparticles. Miyazaki *et al*.,[66] have measured the heat capacity of a giant single crystal of fullerene for the temperature range of 6 to 350 K by adiabatic calorimetry. They have estimated the entropy and enthalpy gain by calculating lattice heat capacity from the contribution of lattice vibrations and molecular librations from the Debye and Einstein function respectively. Boucher *et al*.,[67] have measured the heat capacity of gold-polystyrene nanocomposite from differential scanning calorimeter and they have found that the heat capacity value of gold-polystyrene nanocomposite to increase with the increase in the concentration of gold nanoparticles.

3.4 *Distribution of water molecules*

In the previous sections, structural and thermal properties of the gold-fullerene nanocomposite have been determined and discussed in detail. In this section and in the succeeding sections, hydration properties of the gold-fullerene nanocomposite will be examined and explored in detail. The structure and dynamics of the hydration water around the gold-fullerene nanocomposite will determine their interactions and properties in the aqueous environment and they will have implications in their functions and applications. The detailed investigation on the hydration properties of the gold-fullerene nanocomposite is essential for their material science, electrochemical, biological applications such as molecular recognition, adsorption and binding process involving the aqueous environment. To study the spatial arrangement of the water molecules around the gold-fullerene nanocomposite, radial distribution function (RDF) between the terminal groups and water oxygen atoms is computed and shown in Figure 9. It highlights the formation of well-defined hydration layer around the methyl and hydroxy, gold-fullerene nanocomposite.

The first coordination shell of the methyl system is formed at a radial distance of around 5.4 Å. The most probable position between the terminal methyl groups and the water molecules is around 3.8 Å due to the repulsive hydrophobic force acting between them. The water molecules are arranged in two coordination shells for the hydroxy system. The primary coordination shell is formed around 3.5 Å and the secondary coordination shell is formed around 6.0 Å. The most probable position between the terminal hydroxy groups and the water molecules groups is around 2.7 Å. This shift is due to the propensity of the hydroxy terminal groups to have stronger, attractive, hydrophilic interactions towards the water molecules, coupled with the hydrogen bond interactions between them.

The higher magnitude of the first peak in the RDF of the hydroxy system corresponds to the higher concentration of the water molecules in the hydration shell. Similarly, the lower magnitude of the first peak in the RDF of the methyl system corresponds to the lower concentration of the water molecules in the hydration shell. The properties of the water molecules in the hydration shell of the gold-fullerene nanocomposite is different from that of bulk water. For the further interfacial water-based calculations, we consider two regions of bound water molecules namely Region_1 and Region_2 of the gold-fullerene nanocomposite. The Region_1 and Region_2 denote

the water within 3.5 and 6 Å of the gold-fullerene nanocomposite respectively.

To quantify the population of the water molecules within the hydration shell, number of water molecules within the Region_1 and Region_2 of the gold-fullerene nanocomposite is calculated as a function of time (Figure 10). The average number of water molecules in the Region_1 and Region_2 is evaluated from the last 10 ns of the simulation and they are given in Table 2. The huge difference in the population of the water molecules in the hydration shell of the methyl and hydroxy systems can be clearly seen from Figure 10 and Table 2. The hydration shell of the hydroxy gold-fullerene nanocomposite is denser and strongly hydrated while the hydration shell of the methyl gold-fullerene nanocomposite is thinner and weakly hydrated. This result is consistent with the results obtained from the RDF plot between the terminal groups and water oxygen shown in Figure 9.

To get the quantitative picture of the hydration shell structure, the number of hydrogen bonds in the Region_1 and Region_2 of the gold-fullerene nanocomposite is computed as a function of time and it is shown in Figure 11. The average number of hydrogen bonds in the Region_1 and Region_2 is evaluated from the last 10 ns of the simulation and they are given in Table 2. In this work, hydrogen bonds are counted based on the geometric criterion of the cutoff angle of 30° for the donor–hydrogen–acceptor angle, and a cutoff distance of 3.6 Å for the donor–acceptor distance.

In both the Region_1 and Region_2, the number of hydrogen bonds is larger in the case of the hydroxy gold-fullerene nanocomposite. In the Region_1, the population of the hydrogen bonds in the hydroxy system is 5.5 times larger than that in the methyl system. In the Region_2, the population of the hydrogen bonds in the hydroxy system is 1.3 times larger than that in the methyl system. The larger number of hydrogen bonds in the hydration layer of the hydroxy gold-fullerene composite is essentially due to the intermolecular hydrogen bonds between the hydroxy terminal groups and the water molecules in addition to the intramolecular hydrogen bonds. The hydration shell of the methyl gold-fullerene nanocomposite is thinner and weakly hydrated due to the lesser number of the hydrogen bonds and water molecules.

3.5 *Orientation of water molecules*

The interactions between the gold-fullerene nanocomposite and the interfacial water molecules may induce the ordering of water molecules by rotating their dipole moments. The influence of the hydrophobic and hydrophilic terminal groups on the orientation of water molecules in the interfacial zone can be illustrated from the distribution of water dipole angles displayed in Figure 12. The water dipole angle is defined as the angle between the vector of the dipole of a water molecule and the vector connecting the oxygen atom of a water molecule with the center of the gold-fullerene nanocomposite. For the bulk water, the distribution of water dipole angles will be flat as all the orientations of water molecules are equally probable. The preferred and ordered orientation of the interfacial water molecules of the gold-fullerene nanocomposite is evident from Figure 12. In the methyl system, a single smooth broad peak with the center around 80–90° is observed in both the Region_1 and Region_2. The repulsive interaction between the interfacial water molecules and the hydrophobic surface might have induced this preferential orientation of

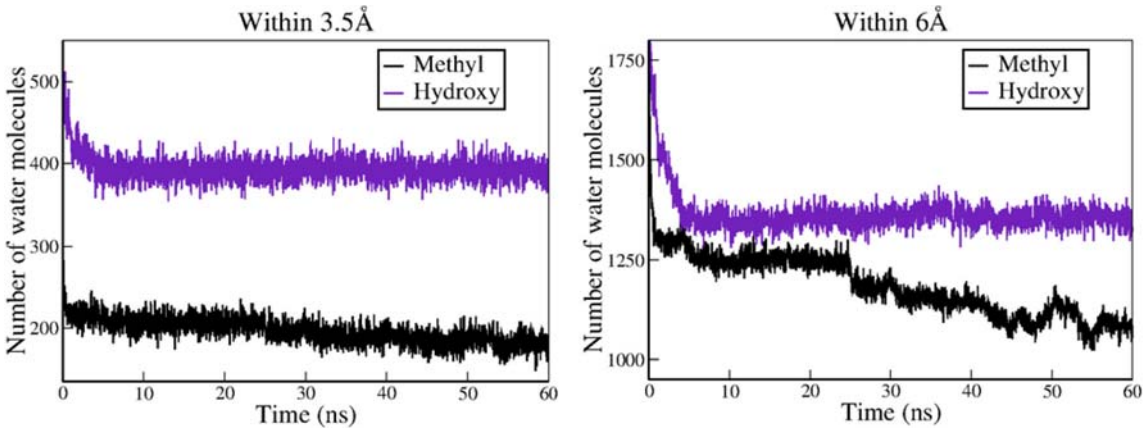

Figure 10. Number of water molecules around gold-fullerene nanocomposite.

Table 2. Hydration properties of gold-fullerene nanocomposite.

Sl. No	Parameter	Methyl	Hydroxy
1	Number of water molecules within 3.5 Å (Region_1)	183 ± 10.79	391 ± 11.65
2	Number of water molecules within 6 Å (Region_2)	1097 ± 31.26	1355 ± 20.47
3	Number of hydrogen bonds within 3.5 Å (Region_1)	28 ± 6.43	153 ± 13.71
4	Number of hydrogen bonds within 6 Å (Region_2)	983 ± 38.23	1263 ± 32.85
5	SASA of nanocomposite ($Å^2$)	10086.12 ± 132.07	10574.11 ± 176.06

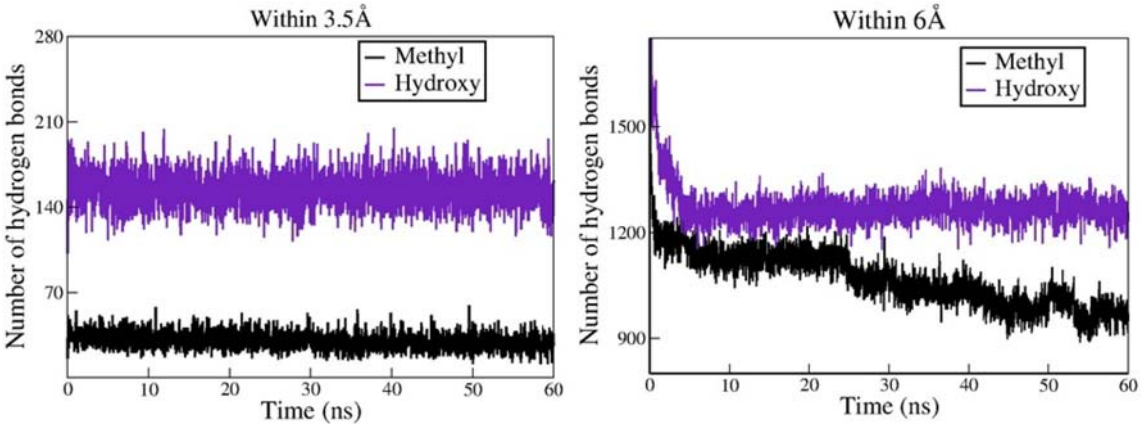

Figure 11. Number of hydrogen bonds around gold-fullerene nanocomposite.

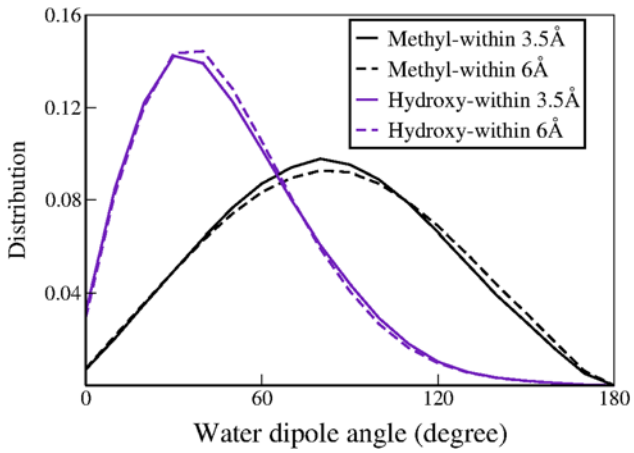

Figure 12. Water dipole angle distribution of gold-fullerene nanocomposite.

water molecules to decrease the surface area of contact with the nanocomposite. In the hydroxy system, most probable water dipole angle is noted around 30–40° in both the Region_1 and Region_2. This biased orientation of the interfacial water molecules towards the attractive hydrophilic functional groups can be attributed to the stronger hydration force, which increases the surface area of contact with the nanocomposite. In the literature, the preferred orientation of the water molecules in the interfacial region of the functionalized gold nanoparticles and fullerene has been reported.[68,69]

3.6 *Water residence time*

The comprehensive understanding of the motion of the water molecules in the vicinity of the nanostructure is essential as they are involved in the various chemical processes and biological activities. The dynamics of the interfacial water molecules of the gold-fullerene nanocomposite has been determined from the residence time correlation function R(t) given in equation (3).

$$R(t) = \left\langle \frac{1}{N} \sum_{i=1}^{N} p_i(t_0) p_i(t_0 + t) \right\rangle \tag{3}$$

In the above equation (3), 'N' represents the number of water molecules residing within the selected water layer, p_i represents the Heaviside step function, which takes the value '1' when a water molecule is present in the selected region in the period $t_0 + t$ and the value '0' otherwise. The residence time correlation function of the water molecules within 3.5 Å (Region_1) and 6 Å (Region_2) of the methyl and hydroxy gold-fullerene nanocomposite is shown in Figure 13. As the

time evolution of the correlation function is biphasic, it is fitted by a double exponential function and the values of the fitted parameters are given in Table 3.

$$R(t) = Ae^{\frac{-t}{\tau_s}} + Be^{\frac{-t}{\tau_l}} \quad (4)$$

In the above equation (4), τ_s and τ_l represent short and long residence time constants. The short residence time constant denotes the librational and vibrational motion of the water molecules.[70,71] The long residence time constant denotes the rotational and translational motion of the water molecules.[70,71]

The integration of residence time correlation function yields average residence time τ

$$\tau = \int_0^\infty R(t)dt \quad (5)$$

The calculated values of the residence time are given in Table 3. The error involved in the calculation of the water residence time is around 5%. The water residence time denotes the measure of the affinity of the water molecules to the surface. In both the Region_1 and Region_2, the water residence time of the hydroxy system is longer than the methyl system. The hydrogen bonds between the hydroxy terminal groups and the water molecules and the stronger attractive interactions between them restrict the mobility of the interfacial water molecules. So the water adsorption is stronger and hence the water stays longer time and their dynamics become slower in the case of the hydroxy gold-fullerene nanocomposite. This observation shows the influence of the chemical functionality of the terminal groups on the dynamics of the hydration water.

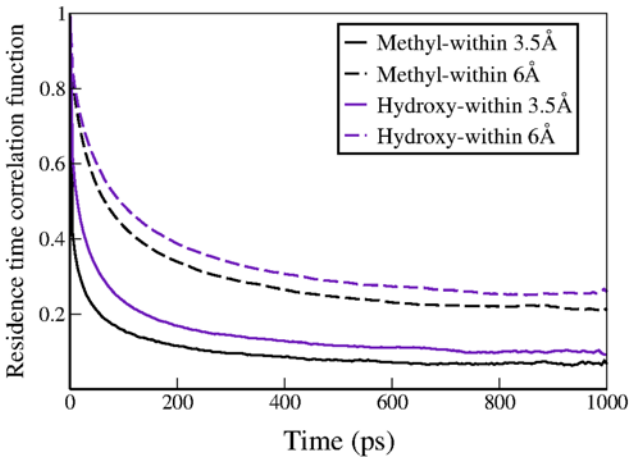

Figure 13. Water residence time correlation function of gold-fullerene nanocomposite.

3.7 *Solvent accessible surface area*

The surface area available for the solvent water molecules to contact the gold-fullerene nanocomposite has been quantified by calculating the solvent-accessible surface area (SASA) for the nanocomposite. We have calculated SASA using the SASA command available in the visual molecular dynamics (VMD) molecular visualization package. We have used a probe radius of 1.4 Å which approximates the radius of a water molecule. In VMD, SASA is calculated using rolling ball algorithm developed by Shrake and Rupley.[72] This numerical method creates a mesh of points representing the surface of each atom at a distance of the van der Waals radius plus the probe radius. Then the number of such mesh points not within the radius of another atom is counted. This number of points is directly proportional to the solvent accessible surface area.

The average SASA values for the methyl and hydroxy, gold nanocomposite calculated from the last 10 ns of the simulation are 10086 and 10574 $Å^2$, respectively (Table 2). The extent to which the gold-fullerene nanocomposite interacts with the water molecules is roughly proportional to the SASA value. The SASA value of the hydroxy gold-fullerene nanocomposite is 488 $Å^2$ higher than the methyl gold-fullerene nanocomposite. The hydrophilic force emerging from the hydroxy terminal moieties has enhanced the exposure surface area of the nanocomposite to the aqueous interface to facilitate their solvation. Lehn *et al.*,[73] have reported the SASA values of mixed-monolayer-protected gold nanoparticles in a

Table 3. Fitting parameters of the time correlation function and water residence time τ.

Parameter	Methyl (Region_1)	Hydroxy (Region_1)	Methyl (Region_2)	Hydroxy (Region_2)
A	0.78	0.61	0.53	0.50
B	0.18	0.21	0.34	0.37
τ_s (ps)	6.32	26.53	62.11	77.52
τ_l (ps)	714.28	1008.71	1858.73	2294.10
τ (ps)	133.50	228.01	664.88	887.56

salt solution to lie in the range of ~18322-18362 Å^2 from their molecular dynamics simulation studies.

The wetting behavior of the methyl and hydroxy gold-fullerene system has been evaluated and examined from the calculation of radial distribution function, number of water molecules, hydrogen bonds, the orientation of water dipoles, water residence time and SASA. All these analyses consistently demonstrate the strongly hydrated interfacial region of the hydroxy gold-fullerene nanocomposite. The enhanced wetting behavior of the hydroxy system is attributed to the stronger, attractive, hydrophilic surface interactions and hydrogen bonding interactions. This result suggests the possibility of controlling the interactions of the gold-fullerene nanocomposite with the water molecules by altering the chemical functionality of their terminal groups.

4. Conclusions

This work presents the structural, thermal and hydration properties of the methyl and hydroxy, gold-fullerene nanocomposite at room temperature, obtained using molecular dynamics simulation technique. The van der Waals interactions between the thiol capped gold nanoparticle and fullerene have driven the formation of the gold-fullerene nanocomposite. The active terminal methyl (hydrophobic) and hydroxy (hydrophilic) groups have influenced the time of formation of self-assembly, stability, conformation and dynamics of the thiol chains, specific heat capacity and hydration properties of the gold-fullerene nanocomposite. The value of the specific heat capacity of the hydroxy gold-fullerene nanocomposite is found to be higher than the methyl gold-fullerene nanocomposite. The variation observed in the specific heat capacity of the gold-fullerene nanocomposite may be attributed to the factors like molecular weight, the conformation of the thiol chains which can vary the frequency of oscillation.

We have predicted the hydration properties of the gold-fullerene nanocomposite such as the structure of hydration layer, the population of interfacial water molecules, hydrogen bonds, the orientation of water molecules, water residence time and solvent accessible surface area. The distribution of the interfacial water molecules is well-structured, bound, ordered with the preferential orientation. When we compare hydroxy and methyl gold-fullerene nanocomposite, the hydroxy system has a strongly hydrated interfacial region with the larger population of water molecules, hydrogen bonds, longer water residence time and higher solvent accessible surface area. This illustrates the enhanced wettability of the hydroxy gold-fullerene nanocomposite. The functionality of the terminal groups has induced the differences in the degree of hydration. Hence the structural, thermal and hydration properties of the gold-fullerene nanocomposite may be modified by the suitable choice of the terminal functional groups. The findings and insights obtained from this simulation study may guide the understanding and development of the gold-fullerene nanostructures, for the future biological, and technological applications, which are based on their structural, thermal and hydration properties. This work can be further extended by simulating the functionalized gold nanoparticle along with the functionalized fullerene and by varying the size of the gold core.

Supplementary information (SI)

Supplementary information contains radial density profile (Figures S1 and S2) of the final structure of methyl and hydroxy gold-fullerene nanocomposite. Supplementary information is available at www.ias.ac.in/chemsci.

Acknowledgements

J. Meena Devi and G. Jayabalaji express their sincere thanks to SERB Fast Track Project [SR/FTP/PS-214/2012], New Delhi, India for the financial support. All the simulations were carried out in High-Performance Computing Cluster at SASTRA Deemed University, Thanjavur, Tamilnadu, India. J. Meena Devi acknowledges the Abdus Salam International Centre for Theoretical Physics (ICTP), Trieste, Italy for providing her Regular Associate award for the period of 01 Jan 2019 to 31 Dec 2024.

References

1. Yeh Y C, Creran B and Rotello V M 2012 Gold nanoparticles: preparation, properties, and applications in bionanotechnology *Nanoscale* **4** 1871
2. Daniel M C and Astruc D 2004 Gold nanoparticles: assembly, supramolecular chemistry, quantum-size-related properties, and applications toward biology, catalysis, and nanotechnology *Chem. Rev.* **104** 293
3. Jin R, Zeng C, Zhou M and Chen Y 2016 Atomically precise colloidal metal nanoclusters and nanoparticles: fundamentals and opportunities *Chem. Rev.* **116** 10346
4. Sardar R, Funston A M, Mulvaney P and Murray R W 2009 Gold nanoparticles: past, present, and future *Langmuir* **25** 13840
5. Gonzalez A L, Noguez C and Barnard A S 2012 Map of the structural and optical properties of gold nanoparticles at thermal equilibrium *J. Phys. Chem. C* **116** 14170
6. Hosseini S, Alsiraey N, Riley A J, Zubkov T, Closson T, Tye J, Bodappa N and Li Z 2018 Variable growth

and characterizations of monolayer-protected gold nanoparticles based on molar ratio of gold and capping ligands *Langmuir* **34** 15517
7. Colangelo E, Comenge J, Paramelle D, Volk M, Chen Q and Levy R 2016 Characterizing self-assembled monolayers on gold nanoparticles *Bioconjug. Chem.* **28** 11
8. Thakor A S, Jokerst J, Zavaleta C, Massoud T F and Gambhir S S 2011 Gold nanoparticles: a revival in precious metal administration to patients *Nano Lett.* **11** 4029
9. Homberger M and Simon U 2010 On the application potential of gold nanoparticles in nanoelectronics and biomedicine *Philos. Trans. R. Soc. A* **368** 1405
10. Ahmad R, Griffete N, Lamouri A, Felidj N, Chehimi M M and Mangeney C 2015 Nanocomposites of gold nanoparticles@ molecularly imprinted polymers: chemistry, processing, and applications in sensors *Chem. Mater.* **27** 5464
11. Sztandera K, Gorzkiewicz M and Klajnert-Maculewicz B 2019 Gold nanoparticles in cancer treatment *Mol. Pharm.* **16** 1
12. Mieszawska A J, Mulder W J, Fayad Z A and Cormode D P 2013 Multifunctional gold nanoparticles for diagnosis and therapy of disease *Mol. Pharm.* **10** 831
13. Nasaruddin R R, Chen T, Yan N and Xie J 2018 Roles of thiolate ligands in the synthesis, properties and catalytic application of gold nanoclusters *Coord. Chem. Rev.* **368** 60
14. Hermanson G T 2013 In *Buckyballs, Fullerenes, and Carbon Nanotubes, Bioconjugate Techniques* 3rd edn. Chapter 16 (Location: Elsevier) p. 741
15. Dinadayalane T C and Leszczynski J 2012 In *Handbook of Computational Chemistry* 1st edn. Chapter 22 (Dordrecht: Springer) p. 793
16. Dinadayalane T C and Leszczynski J 2010 Remarkable diversity of carbon-carbon bonds: structures and properties of fullerenes, carbon nanotubes, and graphene *Struct. Chem.* **21** 1155
17. Goodarzi S, Da Ros T, Conde J, Sefat F and Mozafari M 2017 Fullerene: biomedical engineers get to revisit an old friend *Mater. Today* **20** 460
18. Hirsch A 2010 The era of carbon allotropes *Nat. Mater.* **9** 868
19. Bosi S, Da Ros T, Spalluto G and Prato M 2003 Fullerene derivatives: an attractive tool for biological applications *Eur. J. Med. Chem.* **38** 913
20. Castro E, Garcia A H, Zavala G and Echegoyen L 2017 Fullerenes in biology and medicine *J. Mater. Chem. B* **5** 6523
21. Zhang Y, Murtaza I and Meng H 2018 Development of fullerenes and their derivatives as semiconductors in field-effect transistors: exploring the molecular design *J. Mater. Chem. C* **6** 3514
22. Jariwala D, Sangwan V K, Lauhon L J, Marks T J and Hersam M C 2013 Carbon nanomaterials for electronics, optoelectronics, photovoltaics, and sensing *Chem. Soc. Rev.* **42** 2824
23. Fang Y, Huang Q -J, Wang P, Li X -Y and Yu N -T 2003 Adsorption behavior of C_{60} fullerene on golden crystal nanoparticles *Chem. Phys. Lett.* **381** 255
24. Piotrowski P, Pawlowska J, Pawlowski J, Opuchlik L J, Bilewicz R and Kaim A 2014 Fullerene modification of gold electrodes and gold nanoparticles based on application of aromatic thioacetate-functionalized C60 *RSC Adv.* **4** 64310
25. Matsuo Y, Lacher S, Sakamoto A, Matsuo K and Nakamura E 2010 Conical pentaaryl[60] fullerene thiols: self-assembled monolayers on gold and photocurrent generating property *J. Phys. Chem. C* **114** 17741
26. Lu F, Xiao S, Li Y, Song Y, Liu H, Li H, Zhuang J, Liu Y, Gan L and Zhu D 2004 Fullerene-functionalized gold core–shell nanoparticles: preparation and optical limiting properties *Inorg. Chem. Commun.* **7** 960
27. Luo Z, Zhao Y S, Yang W, Peng A, Ma Y, Fu H and Yao J 2009 Core-shelll nanopillars of fullerene C60/C70 loading with colloidal Au nanoparticles: a Raman scattering investigation *J. Phys. Chem. A* **113** 9612
28. Shi J, Chen Z, Wang L, Wang B, Xu L, Hou L and Zhang Z 2016 A tumor-specific cleavable nanosystem of PEG-modified C60@ Au hybrid aggregates for radio frequency-controlled release, hyperthermia, photodynamic therapy and X-ray imaging *Acta Biomater.* **29** 282
29. Yin G, Xue W, Chen F and Fan X 2009 Self-repairing and superhydrophobic film of gold nanoparticles and fullerene pyridyl derivative based on the self-assembly approach *Colloids Surf. Physicochem. Eng. Asp.* **340** 121
30. Palanisamy S, Thirumalraj B and Chen S -M 2015 Electrochemical fabrication of gold nanoparticles decorated on activated fullerene C60: an enhanced sensing platform for trace level detection of toxic hydrazine in water samples *RSC Adv.* **5** 94591
31. Bonifazi D, Enger O and Diederich F 2007 Supramolecular [60] fullerene chemistry on surfaces *Chem. Soc. Rev.* **36** 390
32. Ahangari M G, Ganji M D and Jalali A 2016 Interaction between fullerene-wheeled nanocar and gold substrate: a DFT study *Phys. E Low-Dimens. Syst. Nano* **83** 174
33. Nemati A, Pishkenari H N, Meghdari A and Sohrabpour S 2018 Directing the diffusive motion of fullerene-based nanocars using nonplanar gold surfaces *Phys. Chem. Chem. Phys.* **20** 332
34. Sändig N, Bakalis E and Zerbetto F 2015 Stochastic analysis of movements on surfaces: the case of C60 on Au (1 1 1) *Chem. Phys. Lett.* **633** 163
35. Pishkenari H N, Nemati A, Meghdari A and Sohrabpour S 2015 A close look at the motion of C60 on gold *Curr. Appl. Phys.* **15** 1402
36. Akimov A V, Williams C and Kolomeisky A B 2012 Charge transfer and chemisorption of fullerene molecules on metal surfaces: application to dynamics of nanocars *J. Phys. Chem. C* **116** 13816
37. Ryu T, Lansac Y and Jang Y H 2017 Shuttlecock-shaped molecular rectifier: asymmetric electron transport coupled with controlled molecular motion *Nano Lett.* **17** 4061
38. Sutradhar S and Patnaik A 2017 Charge transfer-induced assembly of a gold nanocomposite mediated by N-methylfulleropyrrolidine: excitation energy transfer from Rhodamine B *New J. Chem.* **41** 2401
39. Sutradhar S and Patnaik A 2017 Structure and dynamics of a N-methylfulleropyrrolidine-mediated gold

nanocomposite: a spectroscopic ruler *ACS Appl. Mater. Interfaces* **9** 21921
40. Stadler R, Kubatkin S and Bjørnholm T 2007 An ab initio study of the field-induced position change of a C60 molecule adsorbed on a gold tip *Nanotechnology* **18** 165501
41. Chen C -H, Krylov D S, Avdoshenko S M, Liu F, Spree L, Westerström R, Bulbucan C, Studniarek M, Dreiser J and Wolter A U B 2018 Magnetic hysteresis in self-assembled monolayers of Dy-fullerene single molecule magnets on gold *Nanoscale* **10** 11287
42. Wang J, Tang J -M, Larson A M, Miller G P and Pohl K 2013 Sharp organic interface of molecular C60 chains and a pentacene derivative SAM on Au (788): a combined STM & DFT study *Surf. Sci.* **618** 78
43. Bubnis G J, Cleary S M and Mayne H R 2009 Self-assembly and structural behavior of a model rigid C60-terminated thiolate on Au (1 1 1) *Chem. Phys. Lett.* **470** 289
44. Sutradhar S, Jacob G V and Patnaik A 2017 Structure and dynamics of a dl-homocysteine functionalized fullerene-C60–gold nanocomposite: a femtomolar l-histidine sensor *J. Mater. Chem. B* **5** 5835
45. Rincón-García L, Ismael A K, Evangeli C, Grace I, Rubio-Bollinger G, Porfyrakis K, Agraït N and Lambert C J 2016 Molecular design and control of fullerene-based bi-thermoelectric materials *Nat. Mater.* **15** 289
46. Jorgensen W L, Chandrasekhar J, Madura J D, Impey R W and Klein M L 1983 Comparison of simple potential functions for simulating liquid water *J. Chem. Phys.* **79** 926
47. Heinz H, Vaia R A, Farmer B L and Naik R R 2008 Accurate simulation of surfaces and interfaces of face-centered cubic metals using 12-6 and 9-6 Lennard-Jones potentials *J. Phys. Chem. C* **112** 17281
48. Rai B, Sathish P, Malhotra C P, Pradip and Ayappa K G 2004 Molecular dynamic simulations of self-assembled alkylthiolate monolayers on an Au (111) surface *Langmuir* **20** 3138
49. Brooks B R, Bruccoleri R E, Olafson B D, States D J, Swaminathan S and Karplus M 1983 CHARMM: a program for macromolecular energy, minimization, and dynamics calculations *J. Comput. Chem.* **4** 187
50. Devi J M 2014 Aggregation of thiol coated gold nanoparticles: a simulation study on the effect of polymer coverage density and solvent *Comput. Mater. Sci.* **86** 174
51. MacKerell A D Jr, Bashford D, Bellott M, Dunbrack R L Jr, Evanseck J D, Field M J, Fischer S, Gao J, Guo H and Ha S 1998 All-atom empirical potential for molecular modeling and dynamics studies of proteins *J. Phys. Chem. B* **102** 3586
52. Perfilieva O A, Pyshnyi D V and Lomzov A A 2019 Molecular dynamics simulation of polarizable gold nanoparticles interacting with sodium citrate *J. Chem. Theory Comput.* **15** 1278
53. Giri A K and Spohr E 2018 Influence of chain length and branching on the structure of functionalized gold nanoparticles *J. Phys. Chem. C* **122** 26739
54. Velachi V, Bhandary D, Singh J K and Natália M Cordeiro D S 2016 Striped gold nanoparticles: new insights from molecular dynamics simulations *J. Chem. Phys.* **144** 244710
55. Kraszewski S, Tarek M, Treptow W and Ramseyer C 2010 Affinity of C60 neat fullerenes with membrane proteins: a computational study on potassium channels *ACS Nano* **4** 4158
56. Sun Q, Zhang M and Cui S 2019 The structural origin of hydration repulsive force *Chem. Phys. Lett.* **714** 30
57. Yesylevskyy S O, Kraszewski S, Picaud F and Ramseyer C 2013 Efficiency of the monofunctionalized C60 fullerenes as membrane targeting agents studied by all-atom molecular dynamics simulations *Mol. Membr. Biol.* **30** 338
58. Phillips J C, Braun R, Wang W, Gumbart J, Tajkhorshid E, Villa E, Chipot C, Skeel R D, Kale L and Schulten K 2005 Scalable molecular dynamics with NAMD *J. Comput. Chem.* **26** 1781
59. Fujihara H and Nakai H 2001 Fullerenethiolate-functionalized gold nanoparticles: a new class of surface-confined metal-C60 nanocomposites *Langmuir* **17** 6393
60. Bonczak B, Lisowski W, Kaminska A, Holdynski M and Fialkowski M 2019 Gold Nanoparticles functionalized with fully conjugated fullerene C60 derivatives as a material with exceptional capability of absorbing electrons *J. Phys. Chem. C* **123** 6229
61. Velachi V, Bhandary D, Singh J K and Cordeiro M N D 2015 Structure of mixed self-assembled monolayers on gold nanoparticles at three different arrangements *J. Phys. Chem. C* **119** 3199
62. Yu Y, Sun H, Hou T, Wang S and Li Y 2018 Fullerene derivatives act as inhibitors of leukocyte common antigen based on molecular dynamics simulations *RSC Adv.* **8** 13997
63. Balamurugan D, Aquino A J, de Dios F, Flores L Jr, Lischka H and Cheung M S 2013 Multiscale simulation of the ground and photo-induced charge-separated states of a molecular triad in polar organic solvent: exploring the conformations, fluctuations, and free energy landscapes *J. Phys. Chem. B* **117** 12065
64. Natesan H and Bischof J C 2017 Multiscale thermal property measurements for biomedical applications *ACS Biomater. Sci. Eng.* **3** 2669
65. Sauceda H E, Salazar F, Pérez L A and Garzón I L 2013 Size and shape dependence of the vibrational spectrum and low-temperature specific heat of Au nanoparticles *J. Phys. Chem. C* **117** 25160
66. Miyazaki Y, Sorai M, Lin R, Dworkin A, Szwarc H and Godard J 1999 Heat capacity of a giant single crystal of C60 *Chem. Phys. Lett.* **305** 293
67. Boucher V M, Cangialosi D, Alegría A, Colmenero J, Pastoriza-Santos I and Liz-Marzan L M 2011 Physical aging of polystyrene/gold nanocomposites and its relation to the calorimetric T g depression *Soft Matter* **7** 3607
68. Bolintineanu D S, Lane J M D and Grest G S 2014 Effects of functional groups and ionization on the structure of alkanethiol-coated gold nanoparticles *Langmuir* **30** 11075
69. Weiss D R, Raschke T M and Levitt M 2008 How hydrophobic buckminsterfullerene affects surrounding water structure *J. Phys. Chem. B* **112** 2981

70. Hua L, Huang X, Zhou R and Berne B J 2006 Dynamics of water confined in the interdomain region of a multidomain protein *J. Phys. Chem. B* **10** 3704
71. Pal S K, Peon J, Bagchi B and Zewail A H 2002 Biological water: femtosecond dynamics of macromolecular hydration *J. Phys. Chem. B* **106** 12376
72. Shrake A and Rupley J A 1973 Environment and exposure to solvent of protein atoms Lysozyme and Insulin *J. Mol. Biol.* **79** 351
73. Lehn R C V and Alexander-Katz A 2013 Structure of mixed-monolayer-protected nanoparticles in aqueous salt solution from atomistic molecular dynamics simulations *J. Phys. Chem. C* **117** 20104